reduces nitric oxide (NO) activity by activating NADH/NADPH oxidase (*1*), thereby generating superoxide anion ($O_2^{\cdot-}$) according to the reaction NADPH + $2O_2 \rightarrow 2O_2^{\cdot-}$ + $NADP^{+}$ + H^{+}. Found initially in phagocytic cells, NAD(P)H oxidase has also been identified in non-phagocytic cells such as fibroblasts (*2*), endothelial cells (*3*), vascular smooth muscle cells (*4*), renal mesangial cells (*5, 6*), and renal tubular cells (*7, 8*). The upregulation of NAD(P)H oxidase by AII has been demonstrated in aortic vascular smooth muscle (*9, 10*), afferent arterioles of the glomerulus (*11*), and endothelial cells. Reaction between the superoxide anion and nitric oxide will generate peroxynitrite, resulting in oxidative stresses that are highly damaging to endothelial cells. Moreover, studies using chronic kidney disease rodent models have suggested that AII receptor blockade has beneficial effects beyond mere blood-pressure lowering (*12, 13*). It would be of additional interest if AII were to generate superoxide independent of the AII receptor. Therefore, the reduction of AII-mediated oxidative stress presents one approach to control macro-vasculature and micro-vasculature remodeling and endothelial apoptosis (*14*).

Osawa hypothesized in 1970 that fullerenes were the third allotropic carbon form, following graphite and diamond. Because the corannulene molecular structure was a subset of a structure with a soccer ball–like shape, he hypothesized the existence of a full ball (*15*). In 1985, Osawa's prediction—which had been made in a local chemistry journal "*Kagaku*" in Japan and gone mostly unnoticed for over a decade—was rediscovered by Kroto *et al.* (*16*), who began the search anew, and the fullerene was finally isolated in 1990 by Krätschmer *et al.* (*17*). Among fullerenes, C_{60}, or the Buckminsterfullerene, is the smallest. As predicted, it resembles a soccer ball, comprising hexagons and pentagons with no two hexagons sharing an edge. This fullerene is naturally occurring, and commonly found in candle soot. The anti-oxidative potency of native C_{60} fullerenes has been reported by Krusic *et al.* (*18*). The spheroidal structure of C_{60} fullerenes, consisting of numerous interconnected double bonds, is highly reactive with oxygen free radicals. Therefore, the chemical capability to receive oxygen free radicals will be superior to that of known scavengers. Water-soluble fullerenes were first reported by Chiang *et al.* (*19*), Friedman *et al.* (*20*), and Tokuyama *et al.* (*21*). The solubility was secured by either allelic hydroxy or carboxylic acid functional groups synthesized on carbon atoms of the fullerene structure, as seen in fullerenol-1 ($C_{60}(OH)_nO_m$, n=18–20, m=3–7 hemiketal moieties). Subsequently, soluble fullerenes like fullerenol-1 were applied to life sciences. Furthermore, the electric paramagnetic resonance measurement demonstrated that fullerenol-1 virtually abolishes the •OH signal generated by hydrogen peroxide. It is also noteworthy that, by the addition of •OH radicals to the fullerenol-1 molecule, the spheroidal structure of C_{60} provided more stable adducts of C_{60}. In spite of these theoretical aspects implying an inert nature, accumulating evidence supports the notion that fullerenes have prooxidant characteristics (*22–25*). Most of these studies were performed using water-insoluble fullerenes, which are a very different chemical entity from the soluble group, and which must be used with caution due to their toxicity presumably secured during their extraction processes.

Two reports (*26, 27*) have described the anti-oxidative capabilities of water-soluble fullerenes, but none have described a water-soluble fullerene vesicle. Dugan *et al.* investigated the anti-oxidative capacity of water-soluble fullerenes *in vitro* and found that those capabilities differ depending on the chemical structure of the functional group on the surface (*28*). They demonstrated the efficacy of carboxyfullerenes in preventing neuronal death induced by serum deprivation or exposure to Alzheimer amyloid peptide ($A\beta_{1-42}$). We have developed a water-soluble fullerene vesicle of less than 100-nm diameter, which is potentially suitable for endocytotic incorporation, and which is expected to reduce both extracellular and intracellular oxidative stress much more efficiently than previous water-soluble fullerenes. This study, for the first time, examined that antioxidative fullerene-vesicle capability.

Methods

Materials

H_2DCFDA, a "dihydro" derivative of fluorescein, is readily oxidized back to the parent dye, and is thus commonly used as a fluorogenic probe to detect the generation of reactive oxygen species (ROS). A chlormethyl (CM-) derivative of H_2DCFDA, CM-H_2DCFDA, exhibits more specific fluorescence against ROS in live cells than other derivatives, and was therefore used in the present study. CM-H_2DCFDA was obtained from Molecular Probes Inc. (Eugene, USA). Daiichi Sankyo Co. Ltd. (Tokyo, Japan) provided the AII receptor blocker RNH-6270 (RNH; olmesartan) (*29*). For this study, hydroxyphenyl fluorescein (HPF; 2-[6-(4′-hydroxy)phenoxy-3H-xanthen-3-on-9-yl]benzoic acid) was acquired (Daiichi Pure Chemicals Co., Ltd., Tokyo, Japan). HPF does not react with nitric oxide, superoxide, or hydrogen peroxide, and thus responds more specifically to peroxynitrite and hydroxyl radical (*30*). Annexin V and propidium iodide were also obtained from Molecular Probes Inc. Alamar blue was obtained from Biosource International Inc. (Camarillo, USA). The oxidized form of Alamar blue, which has little intrinsic fluorescence, becomes reduced in viable cells. Consequently, the reduced form of Alamar blue is highly fluorescent, and the cellular viability can be quantified by the extent of this conversion. All other chemicals were purchased from Wako Pure Chemical Industries Ltd. (Osaka, Japan) unless otherwise specified.

Fabrication of a Water-Soluble Fullerene Vesicle

The method used to generate water-soluble fullerenes was detailed previously by our group (*31, 32*). In brief, the R

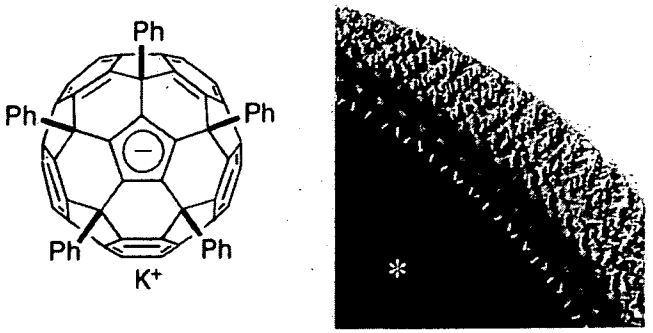

Fig. 1. *Structure of water-soluble fullerene PhK. The three-dimensional structure of fullerene is depicted in the left panel. The estimated outer radius of the fullerene vesicle consisting of PhK is 17.6 nm. Some vesicles shown in the right panel display a bilayer structure in aqueous solution. The asterisk indicates the interior of the fullerene vesicle. Details of the macro-structure are described in our previous report (32).*

(functional group) is substituted with C_6H_5, namely phenyl (penta-) substituted fullerene cyclopentadienide ($Ph_5C_{60}K$, abbreviated as PhK), and attains hydrophobic capabilities. The PhK bilayer vesicle consists of a monoanionic PhK molecule in aqueous solution; its outer shell radius is theoretically calculated as 17.6 nm in water. The micro-chemical structure of PhK is depicted in Fig. 1 (left), along with the putative bilayer structure (right). The structure of the PhK bilayer vesicle was reported previously by our group (*32*).

Cell Culture

Human umbilical venous cells (HUVEC) was obtained from the Health Science Research Resource Bank (HSRRB, Osaka, Japan) and maintained in the defined medium with endothelial supplementation (EGM2 Bullet Kit; Clonetics Corp., San Diego, USA). Endothelial cells were lifted with 0.05% trypsin–0.53 mmol/L EDTA (Gibco BRL, Gaithersburg, USA) and washed. Then 2×10^4 cells/well were seeded in each well of a 96-well plate (Corning Inc., Corning, USA). All experiments were performed using HUVEC between passages 3 and 6.

Cell Viability Assay

The Alamar blue assay is designed to measure cell viability simply, sensitively, and rapidly. The sensitivity and specificity of this dye for measuring cell viability and cytotoxicity are comparable to those of MTT (3-(4,5-dimethylthiazol-2-yl)-2,5-diphenyl-tetrazolium bromide) assay (*33*). Alamar blue is equivalent to non-fluorescent resazurin in oxidized form. Alamar blue appeared very stable in an already "reduced" CO_2-buffered medium. The presence of living cells allowed the reduction of dye through respiration-dependent metabolic activity in which electrons were donated to Alamar blue. The reduced form of Alamar blue is equivalent to resorufin, which has a pinkish fluorescence, and therefore reflects the cellular viability. Among a wide variety of reductases, diaphorase has been identified as the enzyme that is most likely to be responsible for the reduction of resazurin in semen (*34*). Matsumoto *et al.* also demonstrated the diaphorase-dependent reduction of resazurin to resorufin *in vitro* (*35*). Therefore, the level of resofurin will partially reflect the physiological tonus of nitric oxide in endothelial cells.

The HUVEC, seeded in a 96-well microplate (Corning Inc.) at a density of 2×10^4 per well, were capable of creating a cell monolayer after overnight incubation (15 h) and exposure to hydrogen peroxide alone or in combination with the water-soluble fullerene vesicle (PhK) until 8 h of the indicated concentration. To examine cell viability, HUVEC were loaded with 10% Alamar blue. In each experiment, Alamar blue fluorescence was measured on four separate cell monolayers at an excitation wavelength of 544 nm and an emission wavelength of 590 nm using a fluorescent microplate reader (fMax; Molecular Devices Corp., Sunnyvale, USA) and analyzed using software (SoftMax Pro; Molecular Devices Corp.). The experiment was repeated four times. Then HUVEC were preincubated with PhK at 0.1 or 10 μmol/L for 12 h, and subsequently stimulated by the indicated concentration of AII for 8 h. Cellular viability was expressed using the index of percent viability (% viability) against the timed control cells of the same preparation without agonist. A negative control for PhK was established by addition of vehicle (saline) alone instead of PhK. Similarly, RNH was used as a positive control in the AII experiment.

Fluorescence Measurement of Intracellular ROS and Peroxynitrite Production

To measure intracellular ROS production, the HUVEC were loaded on a 96-well fluorescent plate (Corning Inc.) with 10 μmol/L CM-H_2DCFDA for 30 min at 37°C in the dark. Under each experiment, fluorescence of CM-H_2DCFDA was measured on four separate cell monolayers using an excitation

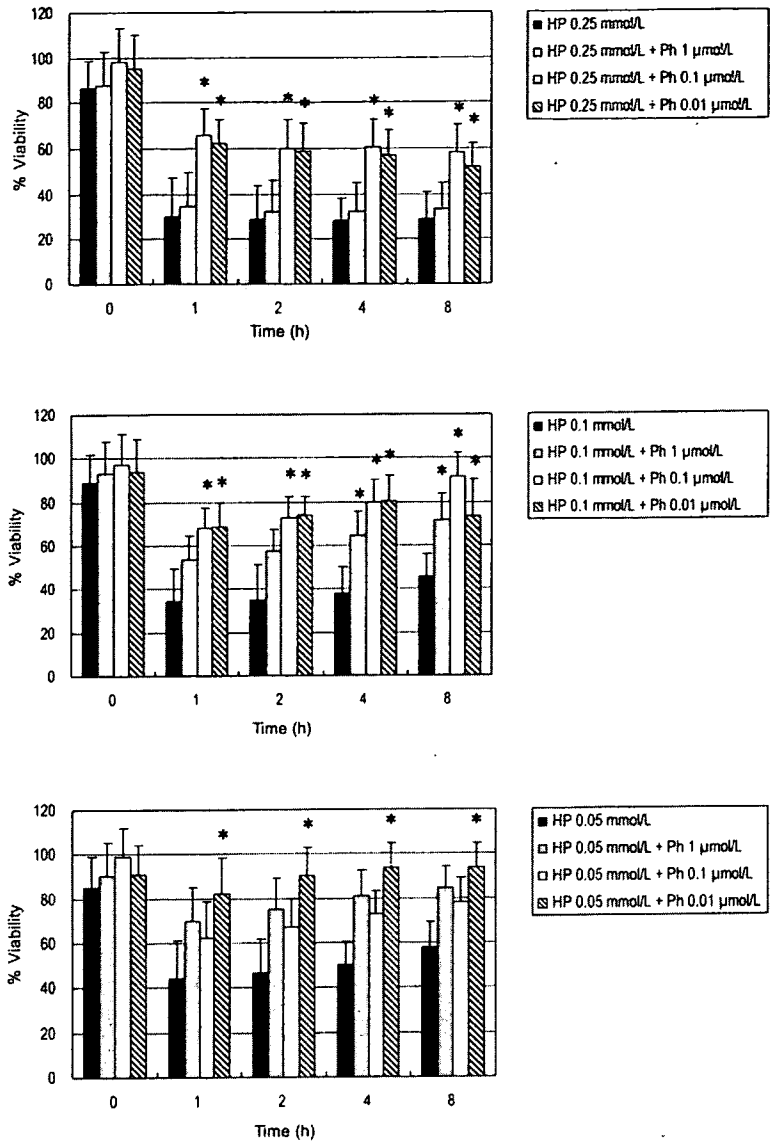

Fig. 2. *PhK improved cellular viabilities against exogenous oxidative stress. Different doses of hydrogen peroxide (HP) and PhK were administered to HUVEC. Cell viabilities were monitored serially at 0, 1, 2, 4, and 8 h time-points. The vertical bar represents % viability. Asterisks denote $p < 0.05$ compared to the positive control.*

wavelength of 485 nm and an emission wavelength of 538 nm with a fluorescence microplate reader (fMax). The HUVEC were exposed to hydrogen peroxide alone at a concentration of 0.10 mmol/L and in combination with fullerenes at concentrations of 0.1 μmol/L, 1 μmol/L, and 10 μmol/L. Experiments were performed for 1 h. Similarly, AII 10^{-7} mol/L was inoculated onto HUVEC after pretreatment with fullerene at the concentrations of 0.1 μmol/L, 1 μmol/L, and 10 μmol/L, as described above, and left for 1 h. The dose-dependency of AII was also monitored for intracellular ROS production. After referring to previous reports of *in vitro* studies, RNH was used at 20 μmol/L concentration (*36–38*). The experiment was repeated four times.

The AII-induced peroxynitrite generation was examined further in HUVEC seeded on a 96-well fluorescent plate. Preincubation of PhK at 0.1 μmol/L or 1 μmol/L was conducted for 12 h, as described above. The peroxynitrite formation was measured using the peroxynitrite-dependent oxidation of dihydrorhodamine-123 to rhodamine-123 using a concentration of 5 μmol/L (*39*). After 24-h incubation, the fluorescence of rhodamine-123 was measured at an excitation wavelength of 500 nm and emission wavelength of 536 nm. Alternatively, peroxynitrite and hydroxyl radical generation were measured using hydroxyphenyl fluorescein (HPF) 10 μmol/L at an excitation wavelength of 485 nm and an emission of 535 nm, where HPF is non-fluorescent until it reacts with the perox-

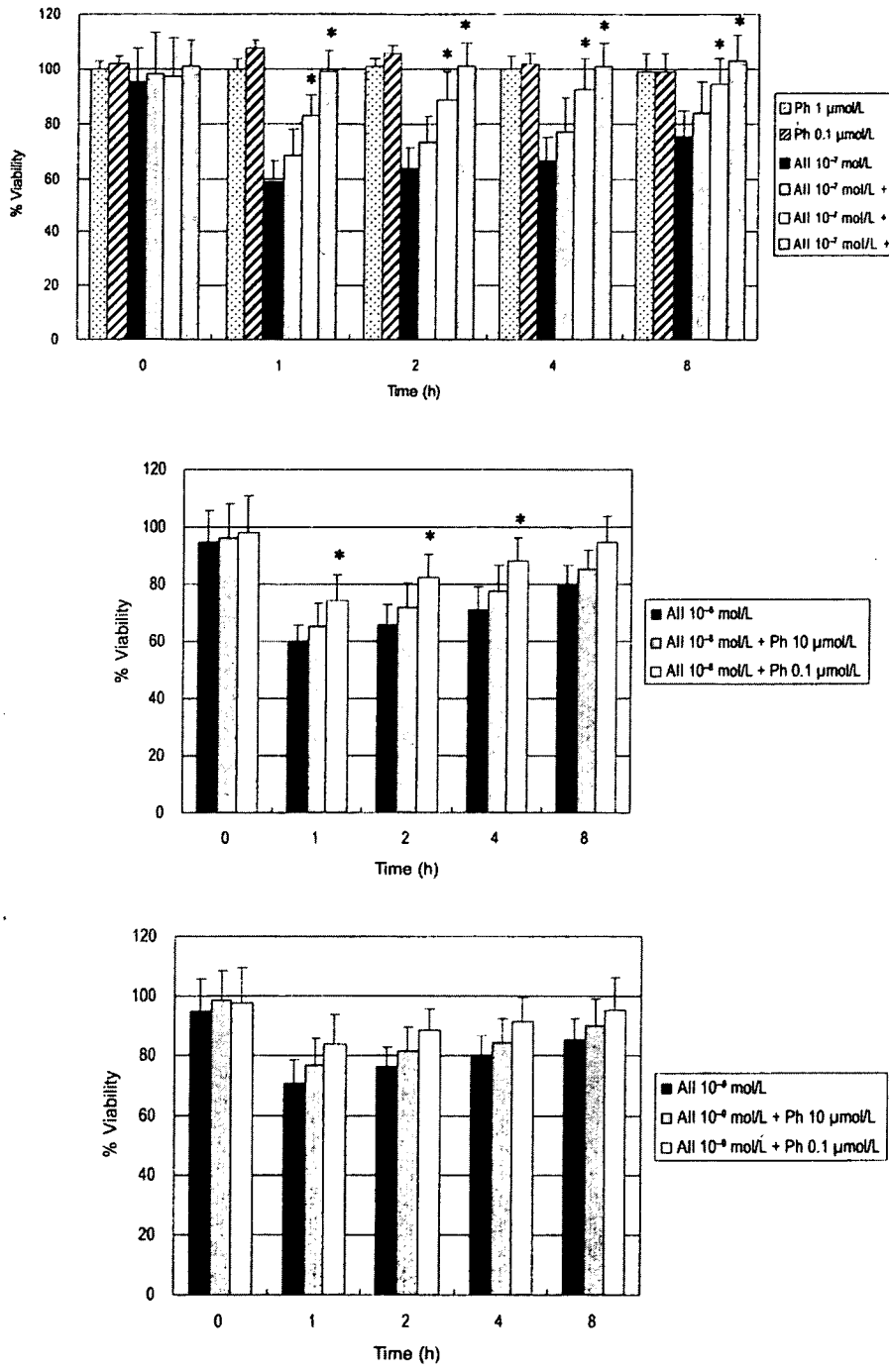

Fig. 3. *PhK improved cellular viabilities against endogenous oxidative stress. Different doses of AII and PhK were administered to HUVEC. Cell viabilities were monitored serially at 0, 1, 2, 4, and 8 h time-points. The vertical bar represents % viabilities. Asterisks denote $p < 0.05$ compared to the positive control.*

ynitrite or related hydroxy radicals. All experiments were performed in quadruplicate, and the experiment was repeated four times.

Flow Cytometry Analysis

Either hydrogen peroxide or AII in combination with PhK was administered to HUVEC monolayers according to the protocols described above. The HUVEC 1×10^6 cells/mL were suspended into 500 μL pre-warmed (37°C) PBS

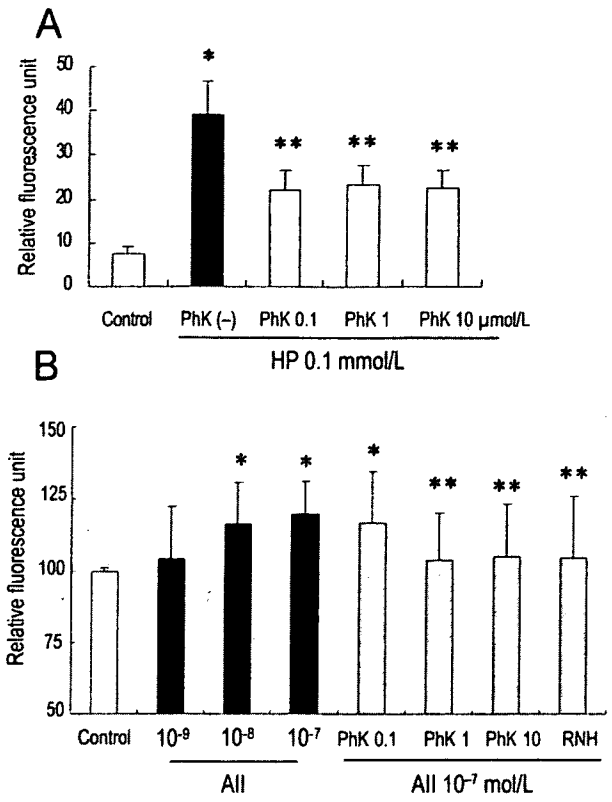

Fig. 4. *PhK reduced exogenous and endogenous oxidative stress. One hour of stimulation with hydrogen peroxide (HP) 0.1 mmol/L was used as an exogenous oxidative stressor (A). Similarly, 1 h of stimulation with the indicated dose of angiotensin II (AII) was used as an endogenous oxidative stressor (B). Exogenous and endogenous ROS were measured using CM-H_2DCFDA. The control cells were treated with vehicle. A single asterisk denotes a significant increase ($p < 0.05$) vs. the control group. The double asterisk denotes a significant decrease ($p < 0.05$) vs. AII 10^{-7} mol/L stimulation.*

(Sigma-Aldrich Corp., St. Louis, USA) supplemented with 5% FBS after trypsinization and washing.

Annexin V 5% was added to the cell suspension, and then incubated at 37°C for 15 min following the manufacturer's instructions. Subsequently, propidium iodide was added at a concentration of 1 μg/mL and flow cytometry was performed using FACScan (BD Biosciences Immunocytometry Systems, San Jose, USA) at a 488 nm excitation wavelength and emission filters of 530 nm (FL-1 channel) and 675 nm (FL-3 channel). Data were analyzed using Cell Quest pro (BD Biosciences). Annexin V detected apoptotic and necrotic cells at the FL-1 high positive area or FL-1 and FL-3 double-positive areas.

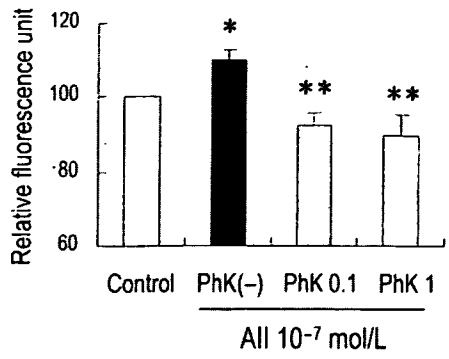

Fig. 5. *AII-induced peroxynitrite and hydroxyl radical generation and the efficacy of PhK. HPF was used for detecting peroxynitrite and/or hydroxyl radical. A single asterisk denotes a significant increase of peroxynitrite generation in the AII without PhK group (PhK(−), $p < 0.05$) compared to the control group. The AII-induced increase of peroxynitrite was alleviated significantly when PhK was added to the medium (double asterisks; $p < 0.05$).*

Preparation for Transmission Electron Microscopic Examination

The HUVEC grown on cover slips to semi-confluence were incubated with PhK 10 μmol/L for 12 h, washed three times using PBS, and fixed using 2.5% glutaraldehyde (Electron Microscopy Sciences, Ft. Washington, USA) for 45 min at 4°C. After washing three times with PBS, samples were immersed in 1.5% oxidized osmium for 1 h at 4°C. Post-fixation was performed using 2% paraformaldehyde with 2.5% glutaraldehyde in PBS (pH 7.1) for 20 min and then the samples were dehydrated. Cells on cover slips were transferred to Epon under mild heating. After ultrathin sectioning and post-fixation by uranium acetate and lead citrate, the transmission electron microscopic (TEM) (H-1000; Hitachi Ltd., Tokyo, Japan) examination was performed.

Immunocytochemical Analysis for Hexanoyl-Lysine Adducts Formation

The HUVEC grown in a slide chamber (BD Falcon, Franklin Lakes, USA) were stimulated using AII 10^{-7} mol/L in the presence or absence of PhK 1 μmol/L. Monoclonal antibody for hexanoyl-lysine (HEL; JaICA, Shizuoka, Japan) adducts was applied to the cell monolayer at a dilution of 1 to 200 after fixation using 2% glutaraldehyde and regular blocking procedures. The following staining was performed using a Vectorstain ABC system (Vector Laboratories Inc., Burlingame, USA). For substrate-chromogen reaction, Vector Red (Vector Laboratories Inc.) was used according to the manufacturer's protocol. Mounted preparations were examined using light microscopy (Nikon E600; Nikon Corp., Tokyo, Japan). Images were captured using a CCD camera

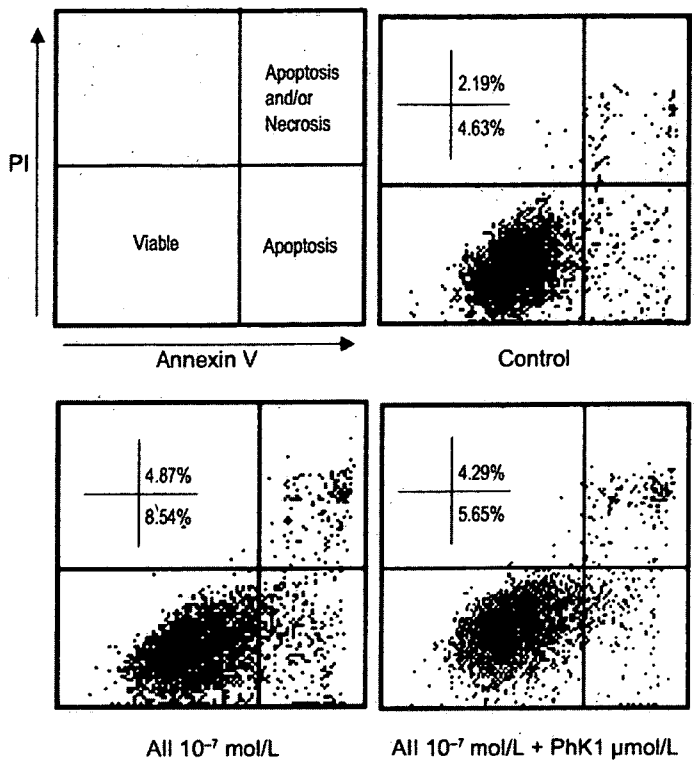

Fig. 6. *AII-induced cellular apoptosis and the efficacy of PhK. The upper left panel shows a map of the cellular distribution. AII 10^{-7} mol/L was added 1 h before measurement. Percentages of "Apoptosis and/or Necrosis" and "Apoptosis" are indicated in each panel.*

(DXM1200F; Nikon Corp., Tokyo, Japan).

Statistical Analyses

The results are expressed as the means±SD. The differences among experimental groups were detected using ANOVA with Tukey's HSD post hoc analysis. Values of $p<0.05$ were considered to indicate statistical significance.

Results

When HUVEC were subjected to exogenous oxidative stress by addition of hydrogen peroxide at concentrations of 0.05 mmol/L, 0.1 mmol/L, and 0.25 mmol/L for 8 h, cellular metabolic viability 1 h after the addition was decreased markedly to about 25% (at 0.25 mmol/L), 35% (0.1 mmol/L), and 45% (0.05 mmol/L) (Fig. 2). These decreases were prolonged for 8 h, but partial improvement in viability was apparent in the hydrogen peroxide 0.05 mmol/L and 0.1 mmol/L groups when PhK was added at a concentration between 0.01 and 1 μmol/L. Similarly, AII-induced reduction of metabolic activity was observed at 2 h after AII addition at concentrations between 10^{-7} and 10^{-9} mol/L (Fig. 3); this decrease was gradually reversed from between 2 and 8 h after AII addition. The decreases in metabolic activity were also greatly ameliorated when the cells were pretreated with PhK at concentrations of 0.1 μmol/L and 10 μmol/L.

The level of oxidative stress was measured using the fluorescent probe CM-H_2DCFDA. Hydrogen-peroxide 0.1 mmol/L–induced ROS were increased markedly from 4.6±0.7 (mean±SD) relative fluorescent units (rfu) in the vehicle group to 39.4±3.6, which was detected clearly using CM-H_2DCFDA. The increase was significantly less ($p<0.01$) for hydorogen peroxide 0.1 mmol/L + PhK 0.1 μmol/L (to 22.4±2.1 rfu), for hydorogen peroxide 0.1 mmol/L + PhK 1 μmol/L (to 23.5±2.2 rfu), and for hydorogen peroxide 0.1 mmol/L + PhK 10 μmol/L (to 22.6±2.2 rfu) (Fig. 4A). Then, AII-induced ROS generation was detected dose-dependently at concentrations of 10^{-7} mol/L and 10^{-9} mol/L using CM-H_2DCFDA. The remarkable increase in ROS production that was apparent in the cells treated with AII 10^{-7} mol/L (to 120.0±11.1 rfu) was reduced considerably by pretreatment with PhK 1 μmol/L (to 103.7±16.6 rfu) or 10 μmol/L (to 105.2±18.0 rfu), and these reduced levels were similar to that following treatment with the AII receptor blocker RNH (104.4±21.5) (Fig. 4B). Furthermore, AII-induced peroxynitrite generation *via* the reaction

$$O_2^{\cdot-} + NO \rightarrow ONOO^{\cdot-}$$

was detected after addition of AII at concentrations between

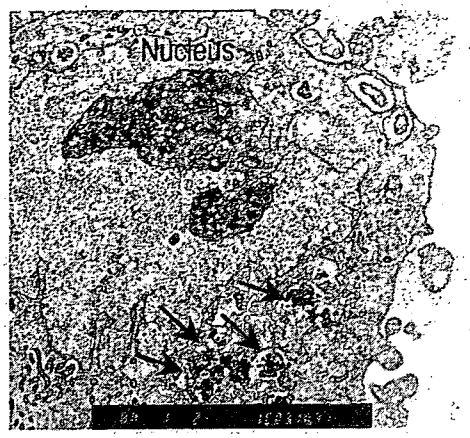

Fig. 7. *Intracellular localization of PhK. This TEM image was captured at 8,000× magnification. Arrows denote electron-dense PhK granules in the cytoplasmic region.*

10^{-7} and 10^{-9} mol/L using rhodamine 123, together with related oxidants. Compared to vehicle-treated cells, peroxynitrite-mediated oxidation was increased 1.9-fold in AII 10^{-7} mol/L–treated cells, 1.7-fold in 10^{-8} mol/L–treated cells, and 1.4-fold in 10^{-9} mol/L–treated cells. These increases were inhibited somewhat by 1 μmol/L PhK: 1.5-fold inhibition was observed in cells treated with AII 10^{-7} mol/L, 1.4-fold inhibition in cells treated with AII 10^{-8} mol/L, and 1.2-fold inhibition in cells treated with AII 10^{-9} mol/L. Next, HPF was used for the AII 10^{-7} mol/L cell preparation as a representative fluorescent indicator for peroxynitrite production. AII 10^{-7} mol/L markedly increased the fluorescence level of HPF, and this increase was decreased significantly by pretreatment with PhK 0.1 μmol/L or 1 μmol/L (Fig. 5).

The combination of Annexin V with propidium iodide is suitable to evaluate apoptosis *in vitro*. Compared to the control, AII 10^{-7} mol/L provoked cellular apoptosis in HUVEC; that induction was reduced by addition of PhK 1 μmol/L (Fig. 6; representative data of three experiments).

Because the AII-induced endogenous oxidative stress was decreased in HUVEC, intracellular incorporation of PhK into HUVEC was investigated using TEM analysis, which clarified the cytoplasmic localization of dense fullerene particles; that image was obtained after 24 h of incubation (Fig. 7).

Typically, ROS will affect the cell membrane, degrading it into arachidonic acid and linoleic acid, where lipid hydroperoxides are formed enzymatically during oxidative stress from 5-lipoxygenase (5-LOX), 15-LOX, cyclooxygenase-1 (COX-1), and COX-2. Both 15-LOX and COX-2 convert linoleic acid into the prototypic *n*-6 polyunsaturated fatty acid (PUFA) hydroperoxide. The major products from oxidized fatty acids are the esterified forms of 9- and 13- hydroxyl/hydroperoxy derivatives of linoleic acid. Furthermore, ROS-derived lipid hydroperoxides break down to form the α,β-unsaturated aldehyde genotoxins, 4-oxo-2-nonenal, 4-hydroxy-2-nonenal, and 4,5-epoxy-2(E)-decenal. Osawa and coworkers recently found that 13-HPODE bound covalently to proteins (*40*). The ROS-derived lipid-hydroperoxides are therefore capable of damaging cellular macromolecules such as DNA and proteins to form HEL, the lipid hydroperoxide–modified lysine residues. A monoclonal antibody raised against HEL adducts is therefore the representative oxidative stress marker for the earlier stages of the lipid peroxidation process. Figure 8 illustrates the AII-induced lipid peroxidation of HUVEC as visualized using anti-HEL antibody. The HEL adducts formation appeared in the cytoplasmic region, as shown in red in the image, when HUVEC were stimulated by AII 10^{-7} mol/L for 3 h. This finding was alleviated in the presence of PhK 1 μmol/L.

Based on the above results, PhK quenched $O_2^{\cdot -}$ derivates from NAD(P)H oxidase, and stopped prolongation of the $O_2^{\cdot -}$-mediated radical chain reaction; reaction with nitric oxide, lipid, mitochondrial DNA, and amino acid in protein. Those quenching will protect cells from apoptosis.

Discussion

This study demonstrated the ability of a water-soluble fullerene vesicle (PhK) to reduce both exogenous and endogenous oxidative stress. Exogenous oxidative stress often occurs with acute injury—*e.g.*, in tissue ischemia reperfusion, multiple organ failure (MOF), and inflammatory diseases such as systemic inflammatory response syndrome (SIRS). Endogenous oxidative stress is more often associated with chronic pathophysiological conditions, which are characterized by chronic endothelial dysfunction in both macro-vascular and micro-vascular systems. This is especially true of such pathophysiological conditions as hypertension, arteriosclerosis, ischemic heart disease, diabetes mellitus, and chronic kidney disease. In other words, endogenous oxidative stress is more closely related to metabolic syndrome and is presumably more important for preventive medicine. Endothelial nitric oxide affects the vasodilation of vascular smooth muscle. The level of endothelial nitric oxide is often mitigated by AII-dependent superoxide generation by NAD(P)H oxidase in endothelial cells (*3*). Consequently, a decrease of nitric oxide by superoxide definitely increases vascular tonus. Therefore, the influence of AII-induced oxidative stress is crucial for control of the diseases described above.

The efficacy of water-soluble fullerenes in reducing oxidative stress has been reported for polyhydroxylated fullerenes, carboxyfullerenes, and hexasulfobutyl[60]fullerenes. Polyhydroxylated fullerenes synthesized by Lai *et al.* were applied to a canine intestinal ischemia-reperfusion model (*41*). Polyhydroxylated fullerenes were effective at decreasing tissue conjugated diene content, which is an index of lipid peroxidation. The tissue malondialdehyde level was also decreased in a polyhydroxylated fullerene group, and the glutathione system was preserved. Similarly, carboxyfullerenes with a very large electronegative center were effective at inhibiting neuronal iron-induced oxidative stress (*42*); hexa-

Fig. 8. *Immunocytochemical detection of HEL induced by AII, and efficacy of PhK. HUVEC stimulated by AII 10^{-7} mol/L for 3 h were examined immunocytochemically using monoclonal anti-HEL antibody. The HEL addcuts formation that was detectable in the cytoplasmic region as red signals was prohibited by administration of PhK 1 μmol/L.*

sulfobutyl[60]fullerenes, which consist of the six sulfobutyl functional group, were protective against oxidation of low-density lipoprotein (*43*). On the other hand, accumulated evidence exists to support prooxidant characteristics of fullerenes (*22–25*). Nonetheless, most of these studies investigated the non water-soluble type. Nagano *et al.* reported singlet oxygen generation from C_{60} fullerenes (*23*), and Satoh *et al.* demonstrated that daimonic acid C_{60} reduces nitric oxide–induced vasodilatation (*24*). Tsuchiya *et al.* reported that the ROS generated by C_{60} interrupts embryonic differentiation, thereby inducing anomalies (*25*); it also exhibits mutagenicity *via* lipid peroxidation (*44*). Furthermore, a recent report from Oberdörster *et al.* suggests the injurious nature of this molecule to marine organisms: they inoculated C_{60} fullerene into water at concentrations of 0.5 ppm and found that largemouth bass suffered a 17-fold increase in lipid peroxidative cellular damage in brain tissue after 48 h (*45*). Clearly, fullerenes have a dual nature, exhibiting both beneficial effects and malign toxicities. Standardization for the material-evaluation of fullerene is therefore required, as we recently suggested (*46*).

The pattern of fullerenes quenching singlet oxygen ($^1O_2$) is chemically dependent on their 30 carbon-carbon double bonds (C=C) (*18, 47*). That mechanism, covalent double bonds reacting with $^1O_2$ through the charge transfer process, is often observed in other well known antioxidants, such as carotenoids (*48–50*) and flavonoids (*51*). In addition, the overall antioxidant and cell-protective capabilities of fullerenes are greater than those of vitamin E (*52*), and the $O_2^{\cdot-}$-quenching capabilities are equivalent to those of ascorbic acid and thiourea (*53*). It is always an issue that these antioxidants exhibit dual characteristics of both free radical generators and quenchers (*54*). Fullerene derivatives are no exception. However, PhK, which has phenyl groups located at the polar head of C_{60}, shows amphiphilicity and produces a bilayer vesicle consisting of 12,700 units of PhK, similar to a lipid bilayer (*32*). In fact, PhK differs from previously reported fullerene derivatives from a structural point of view. The hydrophobic sites, which consist of carbon double bonds and which react with radical species, are secured inside the bilayer (Fig. 1; right). Therefore, if radical chain reactions occur, the reaction might be prolonged inside the vesicle. For that reason, the countervailing radical generator effect that is often seen in antioxidants is inferred to be negligible in PhK.

The cytotoxicity of PhK must be investigated in greater detail in future studies, since PhK can be incorporated into the cytoplasmic region of endothelial cells, as shown by TEM; for that reason, the PhK vesicle might be effective for ameliorating the endogenous oxidative stress induced by AII. We found no cytotoxicity imparted by the dosage of PhK used in this study. The results of this study clarify that PhK is effective for reducing exogenous and endogenous oxidative stress *in vitro*. However, dose-dependency of PhK was not observed within the concentration range used in our experiment. Based on its chemical structure, PhK will never aggregate in pure water within the range of 1 to 10 μmol/L. Nevertheless, the higher electrolyte concentration in culture medium definitely induces aggregation of PhK at the nano-level, which mitigates the higher anti-ROS capability of PhK in higher concentration. For that reason, dose-dependency was not seen in our experiment.

AII-induced superoxide generation is inhibitable by PhK. This capability was shown to be effective at reducing the effects of the earlier stages of the lipid peroxidation process and thereby decreasing the level of cellular apoptosis. Additional studies will be needed to confirm the applicability of PhK to controlling AII-related pathophysiological conditions such as hypertension, atherosclerosis, ischemic heart disease, chronic heart failure, and chronic kidney disease.

References

1. Griendling KK, Minieri CA, Ollerenshaw JD, Alexander RW: Angiotensin II stimulates NADH and NADPH oxidase activity in cultured vascular smooth muscle cells. *Circ Res* 1994; **74**: 1141–1148.
2. Meier B, Jesaitis AJ, Emmendorffer A, *et al*: The cytochrome b-558 molecules involved in the fibroblast and polymorphonuclear leucocyte superoxide-generating NADPH oxidase systems are structurally and genetically distinct. *Biochem J* 1993; **289** (Pt 2): 481–486.
3. Bayraktutan U, Blayney L, Shah AM: Molecular characterization and localization of the NAD(P)H oxidase components gp91-phox and p22-phox in endothelial cells. *Arterioscler Thromb Vasc Biol* 2000; **20**: 1903–1911.
4. Ushio-Fukai M, Zafari AM, Fukui T, *et al*: p22phox is a critical component of the superoxide-generating NADH/NADPH oxidase system and regulates angiotensin II–induced hypertrophy in vascular smooth muscle cells. *J Biol Chem* 1996; **271**: 23317–23321.
5. Radeke HH, Cross AR, Hancock JT, *et al*: Functional expression of NADPH oxidase components (alpha- and beta-subunits of cytochrome b558 and 45-kDa flavoprotein) by intrinsic human glomerular mesangial cells. *J Biol Chem* 1991; **266**: 21025–21029.
6. Jones SA, Hancock JT, Jones OT, *et al*: The expression of NADPH oxidase components in human glomerular mesangial cells: detection of protein and mRNA for p47phox, p67phox, and p22phox. *J Am Soc Nephrol* 1995; **5**: 1483–1491.
7. Hannken T, Schroeder R, Stahl RA, Wolf G: Angiotensin II–mediated expression of p27Kip1 and induction of cellular hypertrophy in renal tubular cells depend on the generation of oxygen radicals. *Kidney Int* 1998; **54**: 1923–1933.
8. Chabrashvili T, Tojo A, Onozato ML, *et al*: Expression and cellular localization of classic NADPH oxidase subunits in the spontaneously hypertensive rat kidney. *Hypertension* 2002; **39**: 269–274.
9. Rajagopalan S, Kurz S, Munzel T, *et al*: Angiotensin II–mediated hypertension in the rat increases vascular superoxide production *via* membrane NADH/NADPH oxidase activation. Contribution to alterations of vasomotor tone. *J Clin Invest* 1996; **97**: 1916–1923.
10. Fukui T, Ishizaka N, Rajagopalan S, *et al*: p22phox mRNA expression and NADPH oxidase activity are increased in aortas from hypertensive rats. *Circ Res* 1997; **80**: 45–51.
11. Wang D, Chen Y, Chabrashvili T, *et al*: Role of oxidative stress in endothelial dysfunction and enhanced responses to angiotensin II of afferent arterioles from rabbits infused with angiotensin II. *J Am Soc Nephrol* 2003; **14**: 2783–2789.
12. Izuhara Y, Nangaku M, Inagi R, *et al*: Renoprotective properties of angiotensin receptor blockers beyond blood pressure lowering. *J Am Soc Nephrol* 2005; **16**: 3631–3641.
13. Sugiyama H, Kobayashi M, Wang DH, *et al*: Telmisartan inhibits both oxidative stress and renal fibrosis after unilateral ureteral obstruction in acatalasemic mice. *Nephrol Dial Transplant* 2005; **20**: 2670–2680.
14. Akishita M, Nagai K, Xi H, *et al*: Renin-angiotensin system modulates oxidative stress–induced endothelial cell apoptosis in rats. *Hypertension* 2005; **45**: 1188–1193.
15. Osawa E: Superaromaticity. *Kagaku* 1970; **25**: 854–863 (in Japanese).
16. Kroto HW, Heath JR, O'Brien SC, *et al*: C60: Buckminsterfullerene, *Nature* 1985; **318**: 162–163.
17. Krätschmer W, Lamb LD, Fostiropoulos K, Huffman DR: Solid C_{60}: a new form of carbon. *Nature* 1990; **347**: 354–358.
18. Krusic P, Wasserman E, Keizer P, *et al*: Radical Reactions of C60. *Science* 1991; **254**: 1183–1185.
19. Chiang LY, Upasani RB, Swirczewski JW: Versatile nitronium chemistry for C60 fullerene functionalization. *J Am Chem Soc* 1992; **114**: 10154–10157.
20. Friedman SH, DeCamp DL, Sijbesma RP, Srdanov G, Wudl F, Kenyon GL: Inhibition of the HIV-1 protease by fullerene derivatives: model building studies and experimental verification. *J Am Chem Soc* 1993; **115**: 6506–6509.
21. Tokuyama H, Yamago S, Nakamura E, *et al*: Photo-induced biochemical activity of fullerene carboxylic acid. *J Am Chem Soc* 1993; **115**: 7918–7919.
22. Krasnovsky AAJ, Foote CS: Time-resolved measurements of singlet oxygen dimol–sensitized luminescence. *J Am Chem Soc* 1993; **115**: 6013–6016.
23. Nagano T, Tanaka T, Mizuki H, Hirobe M: Toxicity of singlet oxygen generated thermolytically in *Escherichia coli*. *Chem Pharm Bull (Tokyo)* 1994; **42**: 883–887.
24. Satoh M, Matsuo K, Kiriya H, *et al*: Inhibitory effects of a fullerene derivative, dimalonic acid C60, on nitric oxide–induced relaxation of rabbit aorta. *Eur J Pharmacol* 1997; **327**: 175–181.
25. Tsuchiya T, Oguri I, Yamakoshi YN, Miyata N: Novel harmful effects of [60]fullerene on mouse embryos *in vitro* and *in vivo*. *FEBS Lett* 1996; **393**: 139–145.
26. Wang IC, Tai LA, Lee DD, *et al*: C_{60} and water-soluble fullerene derivatives as antioxidants against radical-initiated lipid peroxidation. *J Med Chem* 1999; **42**: 4614–4620.
27. Chien CT, Lee PH, Chen CF, *et al*: *De novo* demonstration and co-localization of free-radical production and apoptosis formation in rat kidney subjected to ischemia/reperfusion. *J Am Soc Nephrol* 2001; **12**: 973–982.
28. Dugan LL, Turetsky DM, Du C, *et al*: Carboxyfullerenes as neuroprotective agents. *Proc Natl Acad Sci U S A* 1997; **94**: 9434–9439.
29. Yao L, Kobori H, Rahman M, *et al*: Olmesartan improves endothelin-induced hypertension and oxidative stress in rats. *Hypertens Res* 2004; **27**: 493–500.
30. Setsukinai K, Urano Y, Kakinuma K, *et al*: Development of novel fluorescence probes that can reliably detect reactive oxygen species and distinguish specific species. *J Biol Chem* 2003; **278**: 3170–3175.
31. Burger C, Hao J, Ying Q, *et al*: Multilayer vesicles and vesicle clusters formed by the fullerene-based surfactant C60(CH3)5K. *J Colloid Interface Sci* 2004; **275**: 632–641.
32. Zhou S, Burger C, Chu B, *et al*: Spherical bilayer vesicles of fullerene-based surfactants in water: a laser light scattering study. *Science* 2001; **291**: 1944–1947.
33. O'Brien J, Wilson I, Orton T, Pognan F: Investigation of the Alamar Blue (resazurin) fluorescent dye for the assessment of mammalian cell cytotoxicity. *Eur J Biochem* 2000; **267**:

5421–5426.

34. Zalata AA, Lammertijn N, Christophe A, Comhaire FH: The correlates and alleged biochemical background of the resazurin reduction test in semen. *Int J Androl* 1998; **21**: 289–294.
35. Matsumoto K, Yamada Y, Takahashi M, *et al*: Fluorometric determination of carnitine in serum with immobilized carnitine dehydrogenase and diaphorase. *Clin Chem* 1990; **36**: 2072–2076.
36. Mizuno M, Sada T, Ikeda M, *et al*: Pharmacology of CS-866, a novel nonpeptide angiotensin II receptor antagonist. *Eur J Pharmacol* 1995; **285**: 181–188.
37. Fujiyama S, Matsubara H, Nozawa Y, *et al*: Angiotensin AT_1 and AT_2 receptors differentially regulate angiopoietin-2 and vascular endothelial growth factor expression and angiogenesis by modulating heparin binding-epidermal growth factor (EGF)–mediated EGF receptor transactivation. *Circ Res* 2001; **88**: 22–29.
38. Iwasaki Y, Ichikawa Y, Igarashi O, *et al*: Trophic effect of olmesartan, a novel AT1R antagonist, on spinal motor neurons *in vitro* and *in vivo*. *Neurol Res* 2002; **24**: 468–472.
39. Ischiropoulos H, Gow A, Thom SR, *et al*: Detection of reactive nitrogen species using 2,7-dichlorodihydrofluorescein and dihydrorhodamine 123. *Methods Enzymol* 1999; **301**: 367–373.
40. Kato Y, Mori Y, Makino Y, *et al*: Formation of N^{ε}-(hexanonyl)lysine in protein exposed to lipid hydroperoxide. A plausible marker for lipid hydroperoxide–derived protein modification. *J Biol Chem* 1999; **274**: 20406–20414.
41. Lai HS, Chen WJ, Chiang LY: Free radical scavenging activity of fullerenol on the ischemia-reperfusion intestine in dogs. *World J Surg* 2000; **24**: 450–454.
42. Lin AM, Chyi BY, Wang SD, *et al*: Carboxyfullerene prevents iron-induced oxidative stress in rat brain. *J Neurochem* 1999; **72**: 1634–1640.
43. Lee YT, Chiang LY, Chen WJ, Hsu HC: Water-soluble Hexasulfobutyl[60]fullerene inhibit low-density lipoprotein oxidation in aqueous and lipophilic phases. *Proc Soc Exp Biol Med* 2000; **224**: 69–75.
44. Sera N, Tokiwa H, Miyata N: Mutagenicity of the fullerene C60-generated singlet oxygen dependent formation of lipid peroxides. *Carcinogenesis* 1996; **17**: 2163–2169.
45. Oberdörster E: Manufactured nanomaterials (fullerenes, C60) induce oxidative stress in the brain of juvenile largemouth bass. *Environ Health Perspect* 2004; **112**: 1058–1062.
46. Isobe H, Tanaka T, Maeda R, *et al*: Preparation, purification, characterization, and cytotoxicity assessment of water-soluble, transition-metal–free carbon nanotube aggregates. *Angew Chem Int Ed Engl* 2006; **45**: 6676–6680.
47. Chiang LY, Lu F-J, Lin J-T: Free radical scavenging activity of water-soluble fullerenols. *J Chem Soc Chem Commun* 1995; **12**: 1283–1284.
48. Terao J: Antioxidant activity of beta-carotene–related carotenoids in solution. *Lipids* 1989; **24**: 659–661.
49. Olson JA: Biological actions of carotenoids. *J Nutr* 1989; **119**: 94–95.
50. Krinsky NI: Antioxidant functions of carotenoids. *Free Radic Biol Med* 1989; **7**: 617–635.
51. Korkina LG, Afanas'ev IB: Antioxidant and chelating properties of flavonoids. *Adv Pharmacol* 1997; **38**: 151–163.
52. Emmert DH, Kirchner JT: The role of vitamin E in the prevention of heart disease. *Arch Fam Med* 1999; **8**: 537–542.
53. Sun T, Xu Z: Radical scavenging activities of alpha-alanine C60 adduct. *Bioorg Med Chem Lett* 2006; **16**: 3731–3734.
54. Kawanishi S, Oikawa S, Murata M: Evaluation for safety of antioxidant chemopreventive agents. *Antioxid Redox Signal* 2005; **7**: 1728–1739.